

See discussions, stats, and author profiles for this publication at: <https://www.researchgate.net/publication/8121419>

Binding of recombinant PrPc to human plasminogen: Kinetic and thermodynamic study using a resonant mirror biosensor

ARTICLE *in* PROTEINS STRUCTURE FUNCTION AND BIOINFORMATICS · FEBRUARY 2004

Impact Factor: 2.63 · DOI: 10.1002/prot.20346 · Source: PubMed

CITATIONS

14

READS

28

6 AUTHORS, INCLUDING:



Massimiliano Cuccioloni

University of Camerino

46 PUBLICATIONS 519 CITATIONS

SEE PROFILE



Anna Maria Eleuteri

University of Camerino

64 PUBLICATIONS 1,026 CITATIONS

SEE PROFILE



Simone Barocci

Azienda Sanitaria Unica Regionale, Senigall...

25 PUBLICATIONS 285 CITATIONS

SEE PROFILE



Mauro Angeletti

University of Camerino

107 PUBLICATIONS 1,322 CITATIONS

SEE PROFILE

Binding of Recombinant PrP^c to Human Plasminogen: Kinetic and Thermodynamic Study Using a Resonant Mirror Biosensor

Massimiliano Cuccioloni,^{1*} Manila Amici,¹ Anna Maria Eleuteri,¹ Massimo Biagetti,² Simone Barocci,² and Mauro Angeletti¹

¹MCAB Department, University of Camerino, Italy

²Istituto Zooprofilattico Umbria-Marche, Perugia, Italy

ABSTRACT Transmissible spongiform encephalopathies are a class of sporadic, genetic and transmissible neurodegenerative diseases that affect both humans and animals. Propagation of these diseases is thought to be due to the misfolding of a neuronal glyco-protein, PrP^c, into a pathological insoluble conformer, PrP^{Sc}. In earlier works, some serum components were identified as exclusive PrP^{Sc}-interacting proteins (Fisher et al., *Nature* 2000;408:479), and thus those macromolecules were thought to represent a potential diagnostic endogenous factor discriminating between normal and pathological prion proteins. In contrast, in agreement with a recent work (Kornblatt et al., *Biochem Biophys Res Commun* 2003;305:518), in this paper we present a detailed thermodynamic and kinetic characterization of the interaction between recombinant bovine PrP^c 25–242 and the human serum component plasminogen, measured using a resonant mirror technique: our results reveal a high-affinity interaction between the two binding partners. For comparison, the complex obtained from the purified full-length PrP^c and human plasminogen was also studied: both prion proteins (the recombinant bovine PrP^c 25–242 and the purified full-length PrP^c) are able to bind human plasminogen. Both kinetic and thermodynamic parameters are affected by the modulation exerted by the H⁺ ions in solution. Moreover, the analysis of binding, according to canonical linkage relationships, suggests the involvement of a His residue, consistent with the interaction between other serine (pro)enzymes and their ligands. *Proteins* 2005;58:728–734.

© 2004 Wiley-Liss, Inc.

Key words: prion protein; human plasminogen; biosensor; kinetics; thermodynamics; pH effect

INTRODUCTION

Transmissible spongiform encephalopathies (TSE), or prion diseases, are a class of fatal neurodegenerative disorders affecting both humans and animals. Most of them arise sporadically, some are genetically induced, and a minor ratio can be transmitted between mammals by dietary exposure to, or inoculation with infected tissues.¹

Propagations of the disease are likely to rely only on a structural change in a neuronal glyco-protein,^{2,3} PrP^c which contains two glycosylation sequons in its primary structure. In the disease, the native cellular form, PrP^c, is converted into its insoluble conformer, PrP^{Sc}, containing an increased proportion of β -sheet,⁴ and a proteinase K-resistant core. PrP^{Sc} is thought to replicate by imparting its conformation onto PrP^c.² Prion diseases include bovine spongiform encephalopathies (BSE)⁵ in cattle and scrapie in sheep.⁶ In human prion diseases, such as the Gerstmann-Straussler-Scheinker (GSS) disease,⁷ the kuru,⁸ the fatal familial insomnia,⁹ the sporadic and variant form of Creutzfeldt-Jakob disease,^{10,11} while the conversion of PrP^c to PrP^{Sc} and its accumulation seem to be fundamental events in disease propagation, other aspects of PrP expression, topology, folding and trafficking may be important in the pathological processes which result in disease. The functions of the prion protein are not yet clear, although possible roles in copper transport, synaptic function, circadian rhythm, signal transduction and promotion of genetic diversity have been proposed.^{12–16} TSEs are characterized by a long incubation period, behavioral disturbances, and ataxia, and histologically by a vacuolation of neurons and the neuropil, reactive gliosis, and neuronal loss. In BSE, hydrated autoclaving pretreatment of brain sections before PrP immunolabeling has revealed widespread deposition of abnormal PrP in that organ.¹⁷ Experimental evidence indicates that the aetiology and pathogenesis of TSEs are related at least in part to abnormalities in processing of PrP, constitutively expressed in most tissues but at particularly high levels in the central nervous system.¹⁸ Because deposition of PrP^{Sc} alone is thought not to be a sufficient cause of neuropathology,¹⁹ PrP^{Sc} probably damages the brain by interacting

Abbreviations: NHS, N-hydroxysuccinimide; EDC, 1-ethyl-3-(3-dimethylaminopropyl) carbodiimide; CMD, carboxymethyl-dextran; PMSF, Phenyl-methyl-sulfonyl fluoride; PNGase F, peptide N-glycosidase F; PrP^c, normal cellular prion protein; PrP^{Sc}, scrapie isoform; degly-nPrP^c, deglycosylated native prion protein.

*Correspondence to: Massimiliano Cuccioloni, MCAB Department, University of Camerino, Italy, or Istituto Zooprofilattico Umbria-Marche, Perugia, Italy. E-mail: massimiliano.cuccioloni@unicam.it

Received 11 November 2003; Accepted 3 September 2004

Published online 17 December 2004 in Wiley InterScience (www.interscience.wiley.com). DOI: 10.1002/prot.20346

with other cellular constituents. In published works, some serum components, especially plasminogen, a serum protease implicated in neuronal excitotoxicity,^{20–22} were identified as a PrP^{Sc}-interacting protein and a PrP^c-non-interacting protein. For this reason plasminogen was thought to represent an endogenous factor discriminating between normal and pathological prion proteins. This property might be exploited for diagnostic purpose.²³ In order to better understand the nature of the interaction, in this work we report a detailed study performed with the IAsys resonant mirror biosensor, on the kinetic and thermodynamic parameters characterizing the interaction between human plasminogen and nonglycosylated recombinant PrP^c 25–242, over a wide range of pH.

In agreement with a recent work,²⁴ we show here that in these conditions rec PrP^c 25–242 interacts with immobilized plasminogen.

Moreover, as a validation, purified native full-length PrP^c was tested: the interaction analysis of both prion proteins with human plasminogen resulted in comparable equilibrium dissociation constants.

MATERIALS AND METHODS

Chromatographic Mono-Q (HR 5/5) column and HiTrap chelating column were obtained from Pharmacia-Amersham (Sweden). The CMD cuvette and the NHS immobilization kit, containing NHS, EDC and 1M ethanolamine (pH 8.5) were obtained from Affinity Sensors. Urea, NaOH, NaCl, Tris, KCl, CaCl₂, NaH₂PO₄, obtained from J.T. Baker, Tween-20, MES, CuSO₄, ZW 3-12, sucrose, human plasminogen, PNGase F, PMSF and TPCK obtained from Sigma-Aldrich were of analytical grade. Recombinant PrP^c bovine (25–242) and mouse monoclonal anti-PrP Antibody (mAB) 6H4 were kindly provided by Prionics. FPLC experiments were performed on an AKTA Chromatographic system obtained from Pharmacia-Amersham. Kinetic and thermodynamic studies were performed on an IAsys plus device, Affinity Sensors, obtained from ThermoFinnigan.

Purification of Plasminogen

Human plasminogen was irreversibly inactivated by adding PMSF using a standard procedure.²⁵ The resulting solution was injected on a Mono-Q column and eluted at 0.5 ml/min flow rate with the following segmented gradient of A (Tris-HCl 50 mM, pH 9) and B (Tris-HCl 50 mM, NaCl 1 M, pH 9) buffers: 0–25% B in 8 min, 10 min at 25% B, 25–100% B in 20 min, 8 min at 100% B and finally 100–0% B in 4 min. The plasminogen elution profile shows a sharp single peak: the peak at 17 min, detectable both at 254 and 280 nm, corresponds to plasminogen (Fig. 1).

Purification of PrP^c

PrP^c was purified from bovine brain according to a previously published study.²⁶ Purity of the obtained protein was assessed by standard Western Blot analysis performed with anti-PrP mAB 6H4. Final protein concentration was measured by the optical density at 280 nm using as extinction coefficient a value of 58718.0 M⁻¹cm⁻¹.²⁷

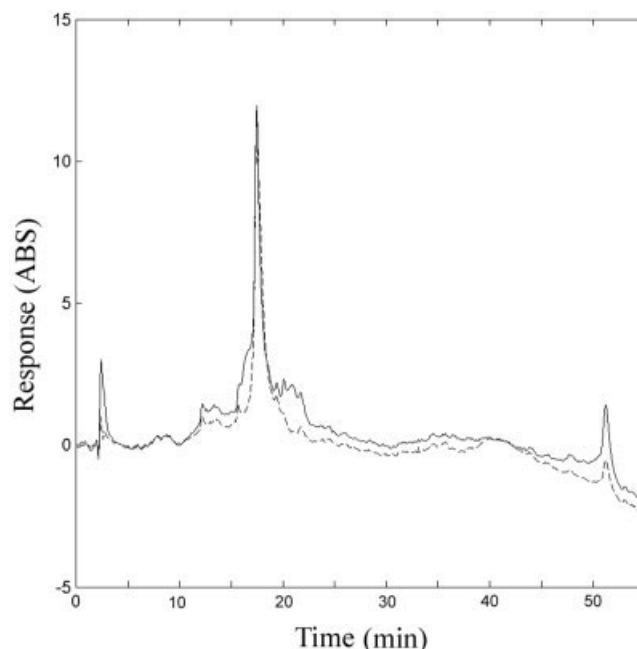


Fig. 1. Elution chromatogram of plasminogen at $\lambda = 254$ nm (dashed line) and $\lambda = 280$ nm (continual line) (see Materials and Methods).

Deglycosylation of PrP^c

Native PrP deglycosylation was performed by overnight incubation with PNGase F at 37°C according to a standard procedure.²⁸

Biosensor Studies

The CMD cuvette was rinsed with PBS-T (NaH₂PO₄ 10 mM, KCl 2.7 mM, NaCl 138 mM, Tween-20 0.05%_(v/v), pH 7.4), and equilibrated with PBS (NaH₂PO₄ 10 mM, KCl 2.7 mM, NaCl 138 mM, pH 7.4) for approximately 10 min to ensure the establishment of a base line for the sensor trace at the set temperature (25°C). Plasmin-free plasminogen was covalently blocked onto the CMD matrix of an IAsys biosensor cuvette by the standard EDC/NHS coupling procedure.²⁹ The noncoupled ligand was removed by washing with PBS buffer for 2 min. Remaining reactive groups were deactivated by a treatment with ethanolamine 1 M, which also assures the removal of any electrostatically bound material. This step was followed by a wash with PBS, a “pulse” wash with HCl 10 mM (regeneration buffer) and one last wash with PBS (Fig. 2).

The amount of immobilized ligand was calculated. A readout of about 500 arcsec was obtained. These conditions resulted in the coupling of a “Langmuir” partial monolayer of a protein of 80 kDa (1 ng/mm² \approx 4 mg/ml). Then, the reaction environment was changed to the desired pH value, and rec PrP^c 25–242 was added at increasing concentrations. These experiments were repeated at different pH conditions. Because repeated regenerations with HCl 10 mM were likely to affect the stability of immobilized plasminogen and its functional ability to interact with soluble rec PrP^c 25–242, regeneration steps were performed with PBS-T instead of HCl 10 mM: in fact, the presence of

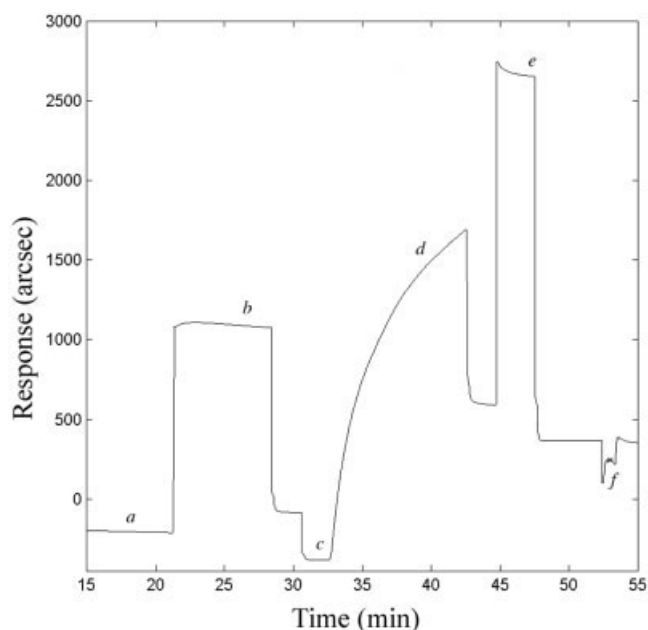


Fig. 2. Immobilization of plasminogen to CMD surface. PBS wash and baseline (a), activation with EDC/NHS (b), change to 10 mM acetate buffer (pH = 6.0) (c), addition of plasminogen (d), blocking with ethanolamine 1M (pH = 8.5) (e), wash with 10 mM HCl (f).

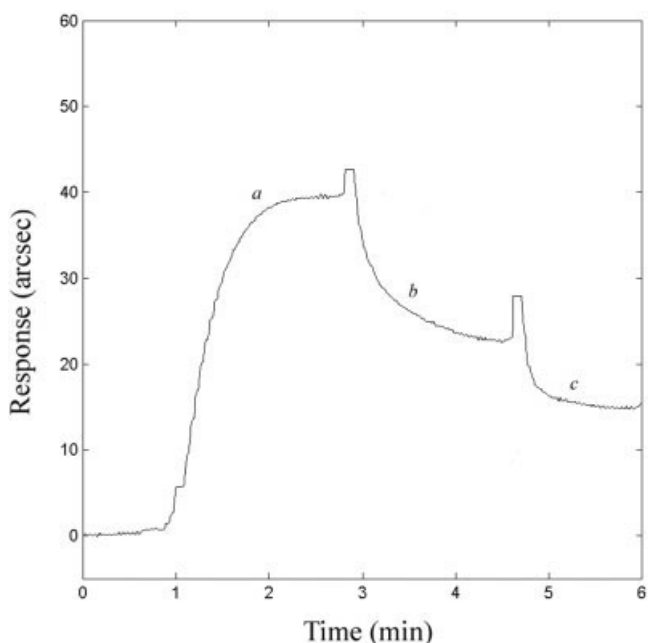


Fig. 3. Rec PrP^c 25–242 binding to immobilized plasminogen: monophasic association (a) and dissociation (b) curve, and regeneration (c).

a detergent is known to affect the binding properties of PrP^c 30 (Fig. 3).

Binding data were analysed using the “Fast Fit software” (Fison Applied Sensor Technology), supplied with the instrument; this program uses an iterative curve-fitting to derive the observed rate constant and the maximum response at equilibrium due to ligand binding at a certain ligand concentration.

RESULTS

Thermodynamics

The pH greatly affects the kinetic association and, less significantly, dissociation properties of the rec PrP^c 25–242 plasminogen recognition process. In fact, the association and dissociation kinetics measured in the range between pH 6.0–8.0 showed different time-courses.

The binding surface containing immobilized plasminogen was obtained as described in Experimental Procedures. The immobilization procedure was optimized after several experiments based upon the variation of plasminogen concentration and immobilization pH value. A plasminogen concentration value of 150 µg/ml and a value of 5.2 for the immobilization pH (chosen on the basis of the plasminogen isoelectric point) were found to best suit a good immobilization of plasminogen while maintaining its functional properties. Under these conditions a final read-out of about 500 arcsec, upon plasminogen immobilization, was obtained. These data were adequate, since immobilization levels should be fairly low for the particular binding studies analyses, in order to minimize steric hindrance and other effects complicating the kinetic analysis.

The binding experiment was repeated at increasing concentrations of rec PrP^c 25–242. At any titration step, baseline achievement was assessed before adding rec PrP^c 25–242, then the regeneration steps were achieved as described in Experimental Procedures. Each binding reaction was followed up to steady state (data not shown). In Figure 4, monophasic association and dissociation time-courses of rec PrP^c binding to immobilized plasminogen are reported.

Equilibrium dissociation constants were calculated for pH values between 6.0 and 8.0. Complex stability shows a bell-shaped curve between pH 6.2 and 7.8: pH dependence of the pK_D shows a maximum at pH 7.2, values ten-fold greater than those measured at pH 6.2 and 7.8, where the curve shows two minima, while at more acidic (or more alkaline) pH values, the pH dependence of the dissociation equilibrium constant increases [Fig. 5(A)]. In addition, binding experiments between native PrP^c purified from bovine brain and plasminogen were performed at pH 7.4 [see Fig. 4(C, D)]. The measured thermodynamic equilibrium constant for the native PrP^c-plasminogen interaction was comparable ($K_{D, \text{recPrP}^c} = [3.39 \pm 0.02] \cdot 10^{-8} \text{ M}$, $K_{D, \text{nPrP}^c} = [1.49 \pm 0.02] \cdot 10^{-8} \text{ M}$) to that obtained for the rec PrP^c.

Kinetics

Calculation of the association (k_{ass}) and dissociation (k_{diss}) rate constants for rec PrP^c 25–242 binding to plasminogen further defines the mechanistic properties of the macromolecular recognition process. The association phase allowed the measurement of the kinetic association constant, while the fast dissociation phase contributed to the high standard deviation associated to the dissociation constant [Fig. 5(D)].

The standard deviations related to each kinetic association constant value k_{ass} (each value was calculated from at least five association/dissociation kinetic experiments) are

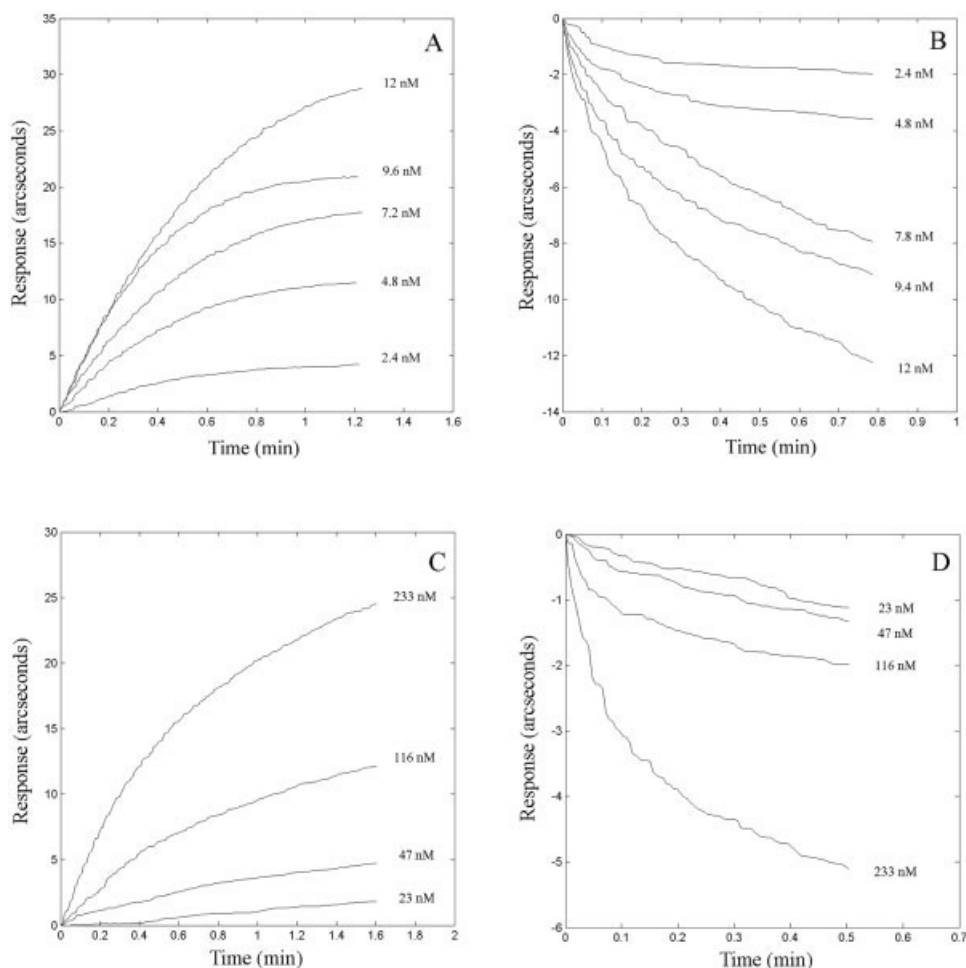


Fig. 4. Rec PrP^c 25–242 and native PrP binding to immobilized plasminogen: overlay of association and dissociation phases measured at increasing concentrations of rec PrP^c 25–242 (A, B) and native PrP^c (C, D), pH = 7.4.

negligible because of the high precision experimental raw data (the instrument short-term noise is less than 1 arcsecond).

Kinetic analysis of the binding of native PrP^c to plasminogen showed a different recognition behavior. These analyses revealed kinetic constant values lower than nonglycosylated rec PrP ($k_{\text{ass,recPrPc}} = [779275.0 \pm 11302.9] \text{ M}^{-1}\text{s}^{-1}$, $k_{\text{ass,nPrPc}} = [98916.1 \pm 134.0] \text{ M}^{-1}\text{s}^{-1}$ and $k_{\text{diss,recPrPc}} = [2.64 \pm 0.14] \cdot 10^{-2} \text{ s}^{-1}$, $k_{\text{diss,nPrPc}} = [1.48 \pm 0.02] \cdot 10^{-3} \text{ s}^{-1}$). Such differences in terms of kinetic association rate constants could be mostly attributed to the large size of the N-linked oligosaccharides present in the native PrP^c surface (the probable glycosylation sites are the Asn 181 and Asn 197).³¹

The carbohydrate moieties in fact shield large exposed regions of the prion protein, covering orthogonal faces of the protein, sterically hindering intramolecular protein–protein interaction¹: this fact could explain the lower association rate exerted by native PrP^c in comparison with rec PrP^c 25–242. On the other hand, the dynamic properties and the flexibility of the oligosaccharidic chains may provide a further anchoring site for the ligands and a route for the protein folding by allowing the protein to interact with other macromolecules, so that the decreased k_{diss} value could be in part explained. Finally, these combined

effects (negative) on the association and (positive) dissociation rates will cancel out and do not affect the thermodynamics of the complex.

The results of the analysis of the interaction between plasminogen and deglycosylated native PrP^c confirms the role of glycosylation on the kinetic and thermodynamic properties of the complex: in fact, such a complex was characterized by kinetic constant values comparable to those obtained for rec-PrP^c ($k_{\text{ass,degly-nPrPc}} = [613374.0 \pm 14111.9] \text{ M}^{-1}\text{s}^{-1}$, $k_{\text{diss,degly-nPrPc}} = [6.97 \pm 0.47] \cdot 10^{-3} \text{ s}^{-1}$), whereas thermodynamics are still not affected ($K_{\text{D,degly-nPrPc}} = [1.14 \pm 0.08] \cdot 10^{-8} \text{ M}$).

The pH dependence of kinetic and thermodynamic constants of the complexes at constant ionic strength was analysed according to earlier studies.³² The theoretical curves shown in Figure 5 were calculated with a nonlinear least-square curve fitting program, from Equations 1 and 2, based on canonical linkage relationships:^{33–35}

$$\log k_{\text{ass,obs}} = \log \frac{k_{\text{ass,0}} + k_{\text{ass,1}}(\lambda_1 + \lambda_3)[\text{H}^+] + k_{\text{ass,2}}\lambda_1\lambda_3[\text{H}^+]}{(1 + \lambda_1[\text{H}^+])(1 + \lambda_3[\text{H}^+])} \quad (1)$$

where the parameters $k_{\text{ass,0}}$, $k_{\text{ass,1}}$, $k_{\text{ass,2}}$ are respectively the rate constants for the unprotonated, single-protonated

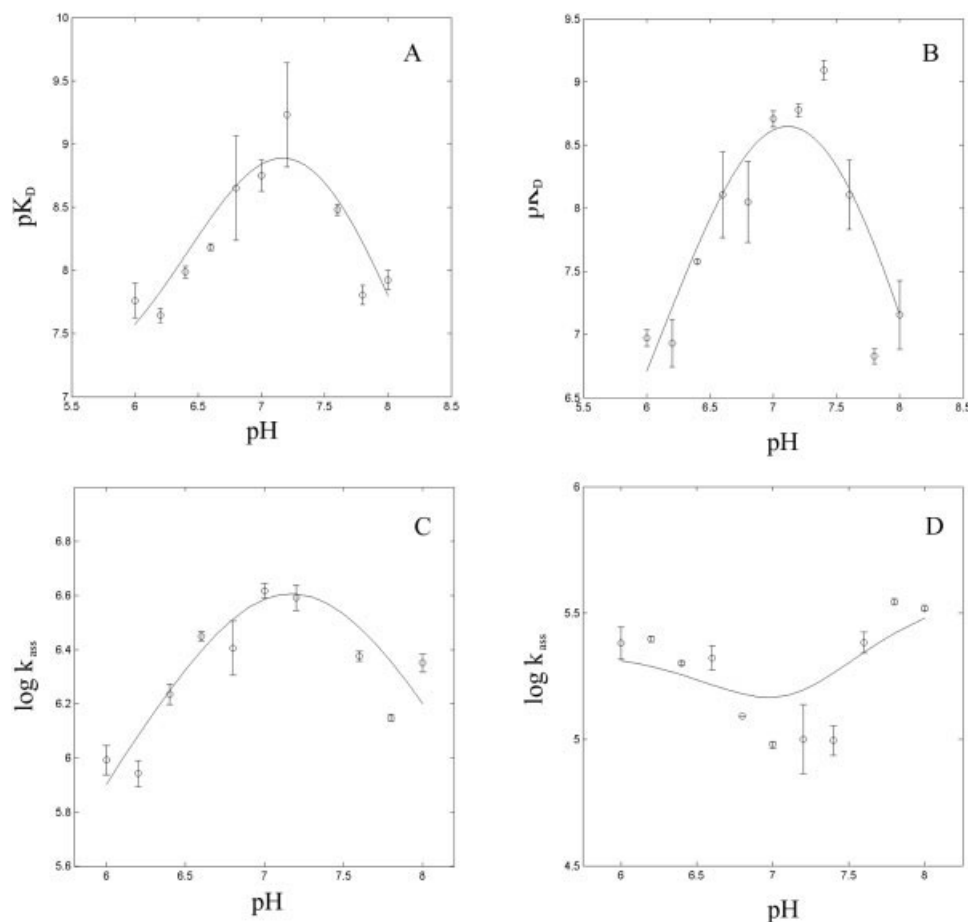


Fig. 5. pH dependence of equilibrium dissociation constants K_D and kinetic association rate constants for the recombinant (A, C) and native prion protein (B, D). The solid lines showed in panels A and B are drawn by using Equation 2, and the solid line showed in C and D are drawn by using Equation 1; the parameters were obtained by nonlinear regression analysis of the experimental data.

and double-protonated species, and λ_1 and λ_3 are the first and the second proton binding constants for the free pro-enzyme.

$$\log K_{D,obs} = \log K_D - \log \left(\frac{(1 + \lambda_1 [H^+])(1 + \lambda_3 [H^+])}{(1 + \lambda_2 [H^+])(1 + \lambda_4 [H^+])} \right)^n \quad (2)$$

The bell-shaped pH-dependency of k_{ass} has a maximum around pH 7.0; it should be noticed that the two macromolecules associate less favorably at pH 6.2 and 7.8. The fast association rates over this pH range suggest that the plasminogen tethering onto the cuvette surface does not affect plasminogen binding to rec PrP^c 25–242.

A simple model for the interpretation of the pH dependence of the kinetic dissociation constants cannot be used; kinetic pH dissociation constant dependence is considerably low all over the pH range of interest and it shows its maximum in the pH range 6.0–6.6, [Fig. 5(C)]. In this pH range, k_{diss} resulted in a particularly high value: in these conditions the dissociation of the complex is kinetically promoted. This is the reason why, instead of a HCl 10-mM regeneration step (it could compromise the functionality or stability of the macromolecule blocked on the cuvette surface), we used a buffered PBS-T solution at pH 6.4:

Tween-20 increased the plasminogen surface regeneration steps.

The bell-shaped pH-dependency of K_D has a maximum around pH 7.4, whereas complex stability is considerably lower at pH 6.2 and 7.8.

DISCUSSION

The experimental results presented in this study show a high affinity interaction between soluble rec PrP^c 25–242 and immobilized plasminogen over a wide pH range, and thus are consistent with the work of Kornblatt et al.²⁴ The interaction is characterized by low equilibrium dissociation constants, mostly due to high association rate constants.

The pH-dependent change in molecular recognition both in k_{ass} and K_D values for rec PrP^c 25–242 binding to plasminogen is strictly reminiscent of that observed for the binding of macromolecular inhibitors (i.e., Kunitz- and Kazal-type inhibitors) to serine (pro)enzymes and thus may be described in similar terms.^{36–42}

The reported data indicate that the different kinetic and thermodynamic parameters can vary substantially as a result of a contained structural perturbation occurring at the interacting surface, which alter the specific recognition contact between plasminogen and rec PrP^c 25–242.

The ionization phenomena that take place on the interface between the proenzyme and rec PrP^c 25–242 seem to be responsible for both the kinetic recognition process and complex stability. The pH dependency of the k_{ass} values for rec PrP^c 25–242-plasminogen complex formation may be attributed to the presence of protonable groups in the free pro-enzyme, characterized by a first proton binding constant $\lambda_1 = 7.24 \pm 0.22$ and a second proton binding constant $\lambda_3 = 7.20 \pm 0.22$. The calculated rate constants, $k_{\text{ass},0} = 1221.01 \pm 56.07 \text{ M}^{-1}\text{s}^{-1}$, $k_{\text{ass},1} = 10964782 \pm 174583 \text{ M}^{-1}\text{s}^{-1}$ and $k_{\text{ass},2} = 1321.03 \pm 109.76 \text{ M}^{-1}\text{s}^{-1}$, revealed that the pro-enzyme single-protonated state is critical to association phase [Fig. 5(B)].

Moreover, the increase in the K_D values for rec PrP^c 25–242 binding to plasminogen on increasing the pH from 6.0 to 7.2, may be interpreted as reflecting the acidic pK-shift of a His residue from $\lambda_1 = 7.24 \pm 0.22$ in the free pro-enzyme, to $\lambda_2 = 6.16 \pm 0.20$ in the plasminogen-rec PrP^c 25–242 complex, most likely corresponding to the His-57 catalytic residue, as seen for other serine (pro)enzymes.^{43–46} The measured acidic pK-shift of the His residue could reflect the burial of the proenzyme active site residue upon complex formation, with change in the local dielectric constant and hydrogen bonds formation.^{33,38,47–49} The calculated λ_3 and λ_4 values ($\lambda_3 = 7.20 \pm 0.22$, $\lambda_4 = 8.65 \pm 0.16$) can be attributed to a terminal α -amino group.

In addition, the analysis of the pH-dependency of K_D for the native PrP^c binding to plasminogen revealed that the glycosylation does not affect considerably the stability of the complex all over the pH range of interest: in fact, the bell shaped pH-dependency of K_D , reminiscent of that observed for rec PrP^c 25–242 binding to plasminogen, may be interpreted in terms of similar pK-shifts from $\lambda_1 = 7.24 \pm 0.22$ in the free enzyme to $\lambda_2 = 6.16 \pm 0.20$ and from $\lambda_3 = 7.20 \pm 0.22$ to $\lambda_4 = 8.54 \pm 0.34$, with $n = 4$ [Fig. 5(B)].

On the other hand, glycosylation considerably affects the plasminogen-native PrP^c recognition process: in fact, the pro-enzyme single-protonated state seems not to favorably recognize native PrP^c ($k_{\text{ass},1} < k_{\text{ass},0}, k_{\text{ass},2}$), with respect to rec PrP^c 25–242 [Fig. 5(D)]. In this work we focused on investigating the thermodynamic and kinetic properties of the interaction between serum component plasminogen and rec PrP^c 25–242 and to this end a resonant mirror biosensor technology has been used; to the best of our knowledge, this is the first time that a resonant mirror has been used to gain quantitative information on the macromolecular recognition process of bovine PrP^c to human plasminogen.

Moreover, in this study both non-glycosylated and glycosylated prion proteins have been used. The glycosyl moiety was thought to take part in the conformational stability of the PrP^c^{50,51} and the interaction with plasminogen was proposed to be conformationally-dependent²³: in this work we quantified the effect exerted by glycosylation on the kinetic properties of the interaction between PrP^c and human plasminogen.

Other systems showed a modulation on binding by glycosyl moiety, although there are no available data on

the effects of glycosylation/deglycosylation on kinetic constants.^{52–56}

Recombinant prion protein shows a functional behavior similar to deglycosylated native full-length prion protein, whereas protein glycosylated native full-length prion protein shows comparable thermodynamic properties, but as a result of the combined effect of decreased association and dissociation rate constants.

Furthermore, these results show the fine modulation of the rec PrP^c 25–242-plasminogen macromolecular recognition process exerted by H⁺ ions. The acid–base equilibria involving amino acid residues at the interface between the pro-enzyme and rec PrP^c 25–242 affect the complex stability association constant in a canonical linkage fashion, while the dissociation constant pH-dependence reveals a singular behavior.

The results obtained could be used in the development of a new biosensor-based diagnostic test in Transmissible Spongiform Encephalopathies via human serum plasminogen as capturing ligand.

ACKNOWLEDGMENTS

This work has been supported in part by a grant from The Italian Ministero della Salute, Ricerca Corrente 2001 “Development of in vivo rapid non-invasive diagnostic strategies for ovine scrapie”. We thank Dr. B. Oesch for providing the Recombinant PrP^c bovine (25–242). We also thank Dr. B. Oesch and Dr. C. Stamm for critical comments and suggestions.

REFERENCES

1. Rudd PM, Wormald MR, Wing DR, Prusiner SB, Dwek RA. Prion glycoprotein: Structure, dynamics, and roles for the sugars. *Biochemistry* 2001;40:3759–3766.
2. Prusiner SB. Novel proteinaceous infectious particles cause scrapie. *Science* 1982;216:136–144.
3. Prusiner SB. Prions. *Proc Natl Acad Sci USA* 1998;95:13363–13383.
4. Pan KM, Baldwin M, Nguyen J, Gasset M, Serban A, Groth D, Mehlthorn I, Huang Z, Fletterick RJ, Cohen PE, Prusiner SB. Conversion of alpha-helices into beta-sheets features in the formation of the scrapie prion proteins. *Proc Natl Acad Sci USA* 1993;90:10962–10966.
5. Wells GAH, Scott AC, Johnson CT, Gunning RF, Bradley R. A novel progressive spongiform encephalopathy in cattle. *Vet Record* 1987;121:419–420.
6. Cuillé, J, Chelle PL. La tremblant du mouton est bien inoculable. *Comptes Rendus de l'Academie des Sciences, Paris* 1939;206:78–79.
7. Gestermann J. Über ein noch beschriebenes Reflexphänomen bei einer Erkrankung des zerebällaren Systems. *Wiener Medizinische Wochenschrift* 1928;78:906–908.
8. Gajdusek DC, Zigas V. Degenerative disease of the central nervous system in New Guinea: The endemic occurrence of kuru in the native population. *N Eng J Med* 1957;257:974–981.
9. Lugaresi E, Medori R, Montagna P, Baruzzi A, Gambetti P. Fatal familial insomnia and dysautonomia with selective degeneration of thalamic nuclei. *N Eng J Med* 1986;315:997–1003.
10. Creutzfeldt HG. Über eine eigenartige herdförmige Erkrankung des Zentral-nervensystems. *Zeitschrift für die gesamte Neurologie und Psychiatrie* 1920;57:78–79.
11. Will RG, Ironside JW, Zeidler M, Cousens SN, Estibeiro K, Alperovitch A, Poser S, Pocchiari M, Hofman A, Smith PG. A new variant of Creutzfeldt-Jakob in the U.K. *Lancet* 1996;347:921–925.
12. Viles JH, Cohen FH, Prusiner SB, Goodin DB, Wright PE, Dyson HJ. Copper binding to the prion protein: structural implications of

- four identical cooperative binding sites. *Proc Natl Acad Sci USA* 1999;96:2042–2047.
13. Collinge J, Whittington MA, Sidle KC, Smith CJ, Palmer MS, Clarke AR, Jefferys JG. Prion protein is necessary for normal synaptic function. *Nature* 1994;370:295–297.
 14. Tobler I, Gaus SE, Deboer B, McBride PA, Manson JC. Altered circadian activity rhythms and sleep devoid prion protein. *Nature* 1996;380:639–642.
 15. True HL, Lindquist SL. A yeast prion provides a mechanism for genetic variation and phenotypic diversity. *Nature* 2000;407:477–482.
 16. Montrasio F, Frigg R, Glatzel M, Klein MA, Mackay F, Aguzzi A, Weissmann C. Impaired prion replication in spleens of mice lacking functional follicular dendritic cells. *Science* 2000;288:1257–1259.
 17. Haritani M, Spencer YI, Wells GA. Hydrated autoclave pretreatment enhancement of prion protein immunoreactivity in formalin fixed bovine spongiform encephalopathy-affected brain. *Acta Neuropathologica (Berlin)* 1994;87:86–90.
 18. DeArmond S, Mobley WC, DeMott DL, Barry RA, Beckstead JH, Prusiner SB. Changes in the localization of brain prion proteins during scrapie infection. *Neurology* 1987;37:1271–1280.
 19. Brandner S, Raeber A, Sailer A, Blatter T, Fisher M, Weissmann C, Aguzzi A. Normal host prion protein necessary for Scrapie-induced neurotoxicity. *Nature* 1996;379:339–343.
 20. Chen ZL, Strickland S. Neuronal death in the hippocampus is promoted by plasmin-catalyzed degradation of lamin. *Cell* 1997;91:917–925.
 21. Tsirka SE, Rogove A, Strickland S. Neuronal cell death and tPA. *Nature* 1996;384:123–124.
 22. Maissen M, Roeckl C, Glatzel M, Goldmann W, Aguzzi A. Plasminogen binds to disease-associated prion protein of multiple species. *Lancet* 2001;357:2026–2028.
 23. Fischer MB, Roeckl C, Parizek P, Schwarz HP, Aguzzi A. Binding of disease-associated prion protein to plasminogen. *Letters to Nature* 2000;408:479–483.
 24. Kornblatt JA, Marchal S, Rezaei H, Kornblatt J, Blany C, Lange R, Debey MP, Hui Bon Hoa G, Marden MC, Grosclaude J. The fate of the prion protein in the prion/plasminogen complex. *Biochem Biophys Res Commun* 2003;305:518–522.
 25. Moss DE, Farhney DE. Kinetic analysis of differences in brain acetylcholinesterase from fish or mammalian sources. *Biochem Pharmacol* 1978;27:2693.
 26. Pan KM, Stahl S, Prusiner SB. Purification and properties of the cellular prion protein from Syrian hamster brain. *Protein Sci* 1992;1:1343–1352.
 27. Rezaei H, Marc D, Choiset Y, Takahashi M, Hui Bon Hoa G, Haertle T, Grosclaude J, Debey P. High Yield purification and physico-chemical properties of full-length recombinant allelic variants of sheep prion protein linked to scrapie susceptibility. *Eur J Biochem* 2000;267:2833–2833.
 28. Zou WQ, Capellari S, Parchi P, Sy MS, Gambetti P, Chen SG. Identification of novel proteinase K-resistant C-terminal fragments of PrP in Creutzfeldt-Jakob. *J Biol Chem* 2003;278(42):40429–40436.
 29. Davies RJ, Edwards PR, Watts HJ, Lowe CR, Buckle PE, Yeung D, Kinning TM, Pollard-Knight DV. The resonant mirror: a versatile tool for the study of biomolecular interactions. In: Crabb JW, editor. *Techniques in protein chemistry*. San Diego: Academic Press; 1994. p 285–292.
 30. Shaked Y, Englestein R, Gabizon R. The binding of prion proteins to serum components is affected by detergent extraction conditions. *J Neurochem* 2002;82:1–5.
 31. Haraguchi T, Fisher S, Olofsson S, Endo T, Groth D, Tarentino A, Borchelt DR, Teplow D, Hood L, Burlingame A, et al. Asparagine-linked glycosylation of the scrapie and cellular prion proteins. *Arch Biochem Biophys* 1989;274:1–13.
 32. Eleuteri AM, Cuccioloni M, Bellesi J, Lupidi G, Fioretti F, Angeletti M. Interaction of HSP90 with 20S proteasome: thermodynamic and kinetic characterization. *Proteins* 2002;49:169–177.
 33. Brocklehurst K, Dixon, HBF. The pH-dependence of second-order rate constants of enzyme modification may provide free-reactant pKa values. *Biochem J* 1977;167:859–862.
 34. Segel, I.H., *Enzyme kinetics, Behavior and analysis of rapid equilibrium and steady-state enzyme systems* New York: Wiley Interscience; 1975.
 35. Wyman J, Gill SJ. *Binding and linkage*. Mid Valley, CA: University Science Books; 1990.
 36. Barrett AJ, Salvensen G. *Proteinase inhibitor*. (eds) Amsterdam: Elsevier; 1986.
 37. Ascenzi P, Coletta M, Amiconi G, Bolognesi M, Menegatti E, Guarneri M. Binding of the bovine basic pancreatic trypsin inhibitor (Kunitz inhibitor) to human and bovine factor Xa. A thermodynamic study. *Biol Chem Hoppe Seyler* 1990;371:389–393.
 38. Amiconi G, Ascenzi P, Bolognesi M, Menegatti E, Guarneri M. Macromolecular biorecognition: principles and methods. In: Chaiken IM, Chiancone E, Fontana A, Neri, P., editors. *Clifton, NJ: Humana Press*; 1988. p 117–130.
 39. Fioretti E, Angeletti M, Passeri D, Ascoli F. Interaction between leukocytic elastase and Kunitz-type inhibitors from bovine spleen. *J Protein Chem* 1989;8:51–60.
 40. Fioretti E, Angeletti M, Cottini MT, Ascoli F. Binding of basic pancreatic trypsin inhibitor and related isoinhibitors to leukocytic elastase. Determination of thermodynamic parameters. *J Mol Recogn* 1989;2:142–146.
 41. Ascenzi P, Aducci P, Amiconi G, Bsillo A, Guadagna A, Menegatti E, Schnebli HP, Bolognesi M. Binding of the recombinant proteinase inhibitor eglin c from leech *Hirudo medicinalis* to serine (pro)enzymes: a comparative thermodynamic study. *J Mol Recogn* 1991;4:113–119.
 42. Ascenzi P, Amiconi G, Coletta M, Lupidi G, Menegatti E, Onesti S, Bolognesi M. Binding of hirudin to human alpha, beta and gamma-thrombin. A comparative kinetic and thermodynamic study. *J Mol Biol* 1992;225:177–184.
 43. Blow DM, Wright CS, Kukla D, Ruhlmann A, Steigemann W, Huber R. A model for the association of bovine pancreatic trypsin inhibitor with chymotrypsin and trypsin. *J Mol Biol* 1972;69:137–147.
 44. Vincent JP, Lazdunski M. The interaction between alpha-chymotrypsin and pancreatic trypsin inhibitor (Kunitz inhibitor). Kinetic and thermodynamic properties. *Eur J Biochem* 1973;38:365–372.
 45. Menegatti E, Guarneri M, Bolognesi M, Ascenzi P, Amiconi G. Binding of bovine basic pancreatic trypsin inhibitor (Kunitz) to human urinary kallikrein and to porcine pancreatic beta-kallikrein A and B. *J Mol Biol* 1984;176:425–430.
 46. Menegatti E, Guarneri M, Bolognesi M, Ascenzi P, Amiconi G. Binding of the bovine basic pancreatic trypsin inhibitor (Kunitz) to human Lys77-plasmin. *J Mol Biol* 1986;191:295–297.
 47. Fioretti E, Angeletti M, Coletta M, Ascenzi P, Bolognesi M, Menegatti E, Rizzi M, Ascoli F. Binding of bovine basic pancreatic trypsin inhibitor (Kunitz) as well as bovine and porcine pancreatic secretory trypsin inhibitor (Kazal) to human cathepsin G: a kinetic and thermodynamic study. *J Enzyme Inhib* 1993;7:57–64.
 48. Bode W, Huber R. Natural protein proteinase inhibitors and their interaction with proteinases. *Eur J Biochem* 1992;204:433–451.
 49. Bode W, Wei AZ, Huber R, Meyer E, Travis J, Neumann S. X-ray crystal structure of the complex of human leukocyte elastase (PMN elastase) and the third domain of the turkey ovomucoid inhibitor. *EMBO J* 1986;5:2453–2458.
 50. Taraboulos A, Rogers M, Borchelt DR, McKinley MP, Scott M, Serban D, Prusiner SB. Acquisition of protease resistance by prion proteins in Scrapie-infected cell does not require asparagine-linked glycosylation. *Proc Natl Acad Sci USA* 1990;87:8262–8266.
 51. Rudd PM, Merry AH, Wormald MR, Dwek RA. Glycosylation and prion protein. *Curr Opin Struct Biol* 2002;12:578–586.
 52. Moller LB, Pollanen J, Ronne E, Pedersen N, Blasi F. N-linked glycosylation of the ligand-binding domain of the human urokinase receptor contributes to the affinity for its ligand. *J Biol Chem* 1993;268:11152–11159.
 53. Akasaki M, Iwata M, Ishizaka K. Modulation of the biologic activities of IgE-binding factors. VII. Biochemical mechanisms by which glycosylation-enhancing factor activates phospholipase in lymphocytes. *J Immunol* 1985;134:4069–4077.
 54. Fischer T, Thoma B, Scheurich P, Pfizenmaier K. Glycosylation of the human interferon-gamma receptor. N-linked carbohydrates contribute to structural heterogeneity and are required for ligand binding. *J Biol Chem* 1990;265:1710–1717.
 55. Krapp S, Mimura Y, Jefferis R, Huber R, Sondermann P. Structural analysis of human IgG-Fc glycoforms reveals a correlation between glycosylation and structural integrity. *J Mol Biol* 2003;325:979–989.
 56. Atsuko Y, Haruko O, Kyoko K, Isamu M. Characterization of the ligand binding activities of vitronectin: interaction of vitronectin with lipids and identification of the binding domains for various ligands using recombinant domains. *Biochemistry* 1998;37:6365–6360.